

Nematic quantum criticality in three-dimensional Fermi system with quadratic band touching

Lukas Janssen and Igor F. Herbut

Department of Physics, Simon Fraser University, Burnaby, British Columbia, Canada V5A 1S6

(Received 1 April 2015; revised manuscript received 17 June 2015; published 20 July 2015)

We construct and discuss the field theory for tensorial nematic order parameter coupled to gapless four-component fermions at the quadratic band touching point in three (spatial) dimensions. Within a properly formulated epsilon-expansion this theory is found to have a quantum critical point, which describes the (presumably continuous) transition from the semimetal into a (nematic) Mott insulator. The latter phase breaks the rotational, but not the time-reversal, symmetry and may be relevant to materials such as gray tin or mercury telluride at low temperatures. The critical point represents a simple quantum analog of the familiar classical isotropic-to-nematic transition in liquid crystals. The properties and the consequences of this quantum critical point are discussed. Its existence supports the scenario of the “fixed-point collision,” according to which three-dimensional Fermi systems with quadratic band touching and long-range Coulomb interactions are unstable towards the gapped nematic ground state at low temperatures.

DOI: [10.1103/PhysRevB.92.045117](https://doi.org/10.1103/PhysRevB.92.045117)

PACS number(s): 71.30.+h, 73.43.Nq, 75.70.Tj

I. INTRODUCTION

Electronic systems that have their Fermi surface reduced to Fermi points recently have received much attention. In particular, recent progress on the problem of interacting Dirac electrons, when the dispersion near the Fermi points is linear in momentum, has indicated that these systems suffer a quantum phase transition with increasing interactions into a gapped phase, described well by the relativistic field theory of the Gross-Neveu-Yukawa type [1]. A weak long-range component of the Coulomb interaction appears to be an irrelevant perturbation at the quantum critical (QC) point, and the transition is essentially due to some of its short-range components becoming sufficiently large. When the dispersion near the Fermi point(s) is quadratic, on the other hand, the result rather differs. In the bilayer graphene, for example, it is one of many possible mass gaps that opens up already at an infinitesimal interaction [2]. The finite density of states that accompanies such a quadratic band touching (QBT) in two dimensions (2D) causes the long-range Coulomb interaction, loosely speaking, to be screened and, at the same time, the noninteracting ground state to be unstable at weak short-range interaction [3,4].

The situation in three-dimensional (3D) systems with QBT is maybe more interesting. QBT arises naturally in many gapless semiconductors, such as gray tin, mercury telluride, or certain pyrochlore iridates [5], that feature band inversion due to spin-orbit coupling. The density of states at the QBT point now vanishes, and the long-range nature of the electron-electron interaction must be taken into account. It has been argued by Abrikosov long ago [6] that the plain vanilla density-density Coulomb interaction in a 3D system with the QBT should turn the ground state into an example of a scale-invariant non-Fermi liquid (NFL). Such an exotic zero temperature phase would manifest itself in characteristic nontrivial power laws in temperature or frequency in various response functions of the system [7].

We have recently pointed out [8], on the other hand, that a 3D system with the chemical potential at the QBT and the Coulomb repulsion between the electrons may be unstable towards an insulating ground state with an anisotropic gap in

the spectrum at low temperatures. The mechanism responsible for this instability was proposed to be the collision between the Abrikosov’s infrared stable NFL fixed point with another, QC, point, which approaches it from the strong-coupling region as the spatial dimensionality of the system is taken to be decreasing from $d = 4$. The collision of fixed points has been studied as a mechanism behind several interesting instabilities in a variety of many-body systems in the past [9–13]. Within the standard one-loop calculation it occurs here somewhat above and close to $d = 3$, when both the NFL and QC fixed points become complex and disappear from the physical space of real couplings. As a result, the coupling constants in the theory run away towards the values at which spontaneous breaking of the rotational symmetry appears to be the most favorable instability. The system in its interacting ground state would effectively appear as if it were under, in this case, *dynamically generated* strain. Furthermore, in the materials with the rest of the band structure equivalent to that of gray tin or mercury telluride as well, the resulting insulating ground state, at least at the mean-field level, would be topologically nontrivial [14]. It therefore would be a precious example of a *topological* Mott insulator [15–18].

In order to remove the Abrikosov’s NFL fixed point, however, the existence of which is guaranteed close to four spatial dimensions, from the physical real-valued space of couplings, it is necessary to have a QC point that would collide with it with the change of some parameter. Indeed, in a certain large- N extension of the theory one can show that such a QC point does exist [8]. At the physical value of $N = 1$, however, in the purely fermionic formulation of the problem the putative QC point lies at strong values of the short-range couplings in the relevant dimensions $3 \leq d < 4$. One may therefore question whether such a QC point is a genuine feature of the theory, and if it would, for example, survive if one went beyond the one-loop approximation. As we will see such reservations would not be entirely without grounds. Similar issue arises in the interacting system of linearly dispersing Dirac fermions [19,20]. In this case, however, an alternative partially bosonized Gross-Neveu-Yukawa formulation can be devised [21]. In this reformulation of the theory one finds a clearly identifiable upper critical dimension, which can be

used to control the quantum critical point and compute its characteristics in perturbative fashion. The crucial ingredient, however, behind this fortunate outcome is the linearity of the Dirac quasiparticle spectrum, which allows the Lorentz symmetry, although absent at the level of the lattice Hamiltonian, to *emerge* dynamically at the QC point. In the systems with the QBT, on the other hand, such an enlarged symmetry is certainly not expected at low energies, and it is *a priori* not even clear what dynamic scaling to assume, as the coupled fermion-boson system on the Gaussian level appears to be characterized by two different dynamical critical exponents, $z = 1$ and 2 , respectively.

Furthermore, as already implicit in Ref. [6] and as will be discussed here at length, one readily finds that the minimal Hamiltonian with the QBT point in 3D requires the use of the maximal set of *five* 4-dimensional mutually anticommuting Dirac matrices. This is not an accident, and the situation is the same in 4D, except that one there needs the maximal set of nine 16-dimensional Dirac matrices. Having no further anticommuting matrix left prohibits then the opening of an isotropic mass gap in the insulating state, which is usually preferred in the systems with Dirac fermions [22,23]. This leaves as the energetically next-best option the dynamical generation of the second-rank tensorial order parameter, which breaks the rotational and preserves the time-reversal symmetry. Such a *nematic* order parameter, as well known from the studies of liquid crystals [24], allows a cubic rotationally invariant term, which is typically responsible for a discontinuous transition. This makes the existence of the QC point in this system seem additionally questionable.

Given these difficulties which appear to be inherent to the problem at hand, it is quite remarkable that together they conspire to allow the construction of the Gross-Neveu-Yukawa type of field theory for the nematic transition in the system with QBT that *has* a perturbatively accessible QC point. We find that it is precisely the presence of the cubic invariant for the nematic order parameter that implies the existence of the upper critical dimension in the theory. The dichotomy in the dynamical scaling of fermions and bosons at the Gaussian fixed point of the theory is naturally resolved at the QC point, with the critical behavior becoming independent of the specific choice of the scaling scheme, and ultimately characterized by a single dynamical critical exponent z . The nematic quantum phase transition from the semimetallic phase into the insulating phase with the anisotropic gap described by the above QC point is therefore presumably *continuous*, at least at the level of the mean-field theory—in contrast to the classical thermal isotropic-to-nematic transition in liquid crystals [24]. To the leading order, the QC point is characterized by the dynamical critical exponent $z = 2$, a nontrivial positive anomalous dimension of the order-parameter field, and a vanishing anomalous dimension for the fermions. The relative signs of the cubic term and the Yukawa couplings at the critical point are also such that the state with fully gapped fermions is favored in the ordered phase, as one would expect from energetics [8].

For the sake of simplicity, in the present work we neglect the effects of the unscreened long-range tail of the Coulomb interaction. While our predictions for the critical exponents near the upper critical dimension may be subject to quantitative

improvement upon its inclusion, possibly already at the leading order in the ϵ expansion, we see no reason why the mechanisms responsible for the *existence* of the nematic QC point should be qualitatively altered when the long-range Coulomb interaction is included—as long as ϵ is small. For larger values of ϵ , in contrast, according to the scenario of the “fixed-point collision” [8], the QBT system with the long-range interaction should become unstable towards an insulating ground state with an anisotropic gap. With the inclusion of the long-range interactions the expansion around the upper critical dimension is thus expected to, even qualitatively, eventually break down at some *lower* critical dimension, which may as well lie above the physical three [8]. Rather than deriving quantitative predictions for experimental systems, our limited objective here is thus to further substantiate the mechanism of “fixed-point collision” by establishing the very existence of the nematic critical point beyond the previous large- N approximation.

The organization of the paper is as follows. In the next section we discuss the construction of the minimal isotropic QBT Hamiltonian in the form that most closely resembles the Dirac Hamiltonian, in general spatial dimension. In Sec. III the Gross-Neveu-Yukawa continuum field theory for the nematic order parameter coupled to fermions is presented. We present the mean-field theory for the nematic quantum phase transition and discuss its order and the nature of the associated interacting ground state in Sec. IV. The structure of the renormalization group and the concomitant quantum critical point are discussed in Sec. V. In Sec. VI we offer an interpretation of our results. Concluding remarks are given in Sec. VII. Some nontrivial technical points necessary for the calculation are presented in five appendices.

II. QBT HAMILTONIANS IN DIFFERENT DIMENSIONS

We first discuss the construction of the minimal, rotationally invariant, and particle-hole symmetric QBT Hamiltonian, in general spatial dimension d . We assume that in the momentum representation it has the form of

$$H = \sum_{i,j=1}^d G_{ij} p_i p_j, \quad (1)$$

with G_{ij} as the matrix coefficients, which need to be determined. Obviously, G_{ij} must transform as the components of a second-rank symmetric tensor under rotations. For simplicity, we set the effective band mass to $2m = 1$ and demand that $H^2 = p^4 \mathbb{1}$, with the minimal dimension of the Hamiltonian to be determined. H^2 thus contains only even powers of the momentum’s components p_i , and the matrix coefficients must then satisfy the anticommutation rules

$$\{G_{\text{of}}, G'_{\text{of}}\} = \{G_d, G_{\text{of}}\} = 0, \quad (2)$$

where G_d is any of the diagonal elements G_{ii} , G_{of} is any of the off-diagonal element G_{ij} with $i \neq j$, and $G_{\text{of}} \neq G'_{\text{of}}$. Then

$$H^2 = \sum_{i=1}^d G_{ii}^2 p_i^4 + \sum_{i<j} p_i^2 p_j^2 (4G_{ij}^2 + \{G_{ii}, G_{jj}\}). \quad (3)$$

If we normalize the diagonal elements so all $G_d^2 = 1$, $H^2 = p^4$ provided that the following condition is satisfied:

$$4G_{\text{of}}^2 + \{G_d, G'_d\} = 2. \quad (4)$$

Demanding further that the tensor G_{ij} is traceless, the Hamiltonian H would contain only the irreducible tensor $p_i p_j - \delta_{ij} p^2/d$ and would be without the scalar term $\propto p^2$. The existence of such a scalar part would only introduce different curvatures of the upper and the lower branches of the energy spectrum, and we omit it for the time being. We therefore set

$$\sum_{i=1}^d G_{ii} = 0, \quad (5)$$

with the spectrum being quadratic, isotropic, and particle-hole symmetric, $\varepsilon_{\pm}(\vec{p}) = \pm p^2$. Tracelessness, however, implies that, for arbitrary index k ,

$$0 = \left\{ G_{kk}, \sum_{i=1}^d G_{ii} \right\} = 2 + \sum_{i(\neq k)} \{G_{kk}, G_{ii}\} \quad (6)$$

or, in other words, that for any pair of diagonal elements

$$\{G_d, G'_d\} = \frac{2}{1-d}. \quad (7)$$

When combined with Eq. (4) this in particular implies that off-diagonal elements are to be normalized as $G_{\text{of}}^2 = d/[2(d-1)]$.

To construct the desired Hamiltonian H we therefore need

$$\left(\frac{d^2 - d}{2} \right) + (d-1) \quad (8)$$

mutually anticommuting Dirac matrices, for the off-diagonal (first) and the diagonal (second term) elements. From $d-1$ Dirac matrices for the diagonal matrices, d matrices G_{ii} that satisfy Eq. (7) and square to unity can always be constructed.

For example:

(1) In $d=2$ only two anticommuting matrices are needed, and therefore they may be chosen as $G_{12} = G_{21} = \sigma_1$ and $G_{11} = -G_{22} = \sigma_3$. The Hamiltonian describes the band touching point in bilayer graphene, for example. Note that H is time-reversal symmetric, and the time-reversal operator is $T = K$, the complex conjugation alone. Since $T^2 = 1$ this Hamiltonian can arise as a low-energy limit of a lattice Hamiltonian with spinless fermions hopping between sites [25]. Examples of such lattice Hamiltonians already exist in the literature [3,4].

(2) In $d=3$ one needs *five* Dirac matrices for the construction, so their minimal dimension is four. We can choose $G_{12} = (\sqrt{3}/2)\gamma_2$, $G_{13} = (\sqrt{3}/2)\gamma_3$, $G_{23} = (\sqrt{3}/2)\gamma_4$, and then for the diagonal elements

$$G_{11} = -\frac{1}{2}\gamma_5 + \frac{\sqrt{3}}{2}\gamma_1, \quad (9)$$

$$G_{22} = -\frac{1}{2}\gamma_5 - \frac{\sqrt{3}}{2}\gamma_1, \quad (10)$$

$$G_{33} = \gamma_5. \quad (11)$$

The Hermitian Dirac matrices γ_a , $a = 1, \dots, 5$ satisfy the Clifford algebra $\{\gamma_a, \gamma_b\} = 2\delta_{ab}$. With this particular choice

the Hamiltonian can also be rewritten as

$$H = \sum_{a=1}^5 d_a(\vec{p})\gamma_a, \quad (12)$$

where $d_a(\vec{p}) = p^2 \tilde{d}_a(\theta, \varphi)$ are proportional to five real spherical harmonics for the angular momentum of $2\omega_0$; explicitly, $\tilde{d}_1 + i\tilde{d}_2 = (\sqrt{3}/2)\sin^2(\theta)e^{2i\varphi}$, $\tilde{d}_3 + i\tilde{d}_4 = (\sqrt{3}/2)\sin(2\theta)e^{i\varphi}$, $\tilde{d}_5 = (3\cos^2\theta - 1)/2$, with θ and φ as the spherical angles in the momentum space.

Note that among the five four-dimensional Dirac matrices we can always choose two (say γ_4 and γ_5) as imaginary and the remaining three as real, so H is also time-reversal invariant, but now with (unique) $T = \gamma_4\gamma_5K$ [25]. Most importantly, $T^2 = -1$, and in three dimensions H inevitably describes particles with half-integer spin. In fact this ‘‘Luttinger Hamiltonian’’ is well known to arise from the spin-orbit coupling in gapless semiconductors such as gray tin, for example [26,27]. Also, the Kramers theorem applies in this case and dictates that the spectrum is doubly degenerate at any momentum.

(3) For completeness, let us also display the solution for $d=4$. For the off-diagonal elements we now need six mutually anticommuting matrices and for the diagonal elements three more. The nine-component Clifford algebra has the unique irreducible representation being 16 dimensional. We may then choose the off-diagonal elements as $(G_{12}, G_{13}, G_{23}, G_{14}, G_{24}, G_{45}) = \sqrt{2}/3(\gamma_2, \gamma_3, \gamma_4, \gamma_6, \gamma_7, \gamma_8)$, and the diagonal elements as

$$G_{11} = -\frac{1}{3}\gamma_9 - \frac{\sqrt{2}}{3}\gamma_5 + \sqrt{\frac{2}{3}}\gamma_1, \quad (13)$$

$$G_{22} = -\frac{1}{3}\gamma_9 - \frac{\sqrt{2}}{3}\gamma_5 - \sqrt{\frac{2}{3}}\gamma_1, \quad (14)$$

$$G_{33} = -\frac{1}{3}\gamma_9 + \frac{\sqrt{8}}{3}\gamma_5, \quad (15)$$

$$G_{44} = \gamma_9. \quad (16)$$

Displaying H in the form equivalent to Eq. (12) would define the four-dimensional generalization of the $\ell=2$ spherical harmonics. Note also that among the nine 16-dimensional Dirac matrices, four (say with indices $a=6,7,8,9$) can be chosen to be purely imaginary, with the remaining five then as real [28]. The time-reversal operator that commutes with H exists and is unique: $T = \gamma_6\gamma_7\gamma_8\gamma_9K$, but again $T^2 = +1$, and the minimal Hamiltonian in $d=4$, similarly to $d=2$, describes a spinless particle.

The solutions to the above conditions for the matrices G_{ij} can be found in all dimensions, with the properties of the minimal Hamiltonian under time reversal, for example, being strongly dimension dependent, as our examples already illustrate. Further details on the construction of the d -dimensional QBT Hamiltonian are provided in Appendix B. The construction can also be generalized to higher-order band touching, which would involve the higher-rank tensors and higher-angular-momentum spherical harmonics. Further elaboration of this point would be somewhat tangential to our main subject, and we leave it for another occasion.

III. THE GROSS-NEVEU-YUKAWA FIELD THEORY

We consider next the QBT fermions in $d = 3$ and at $T = 0$. The system may possibly harbor several QC fixed points which for large-enough short-range interactions could lead to various different instabilities and corresponding symmetry-breaking patterns, in analogy to the 2D Dirac system describing interacting fermions on the honeycomb lattice [20]. Due to the vanishing density of states at the QBT point in 3D any such QC point will be located at strong coupling—as long as the long-range tail of Coulomb interaction is suppressed. With the long-range interaction included, however, the critical coupling is expected to decrease significantly and might even vanish completely [8], in contrast to the Dirac systems. We have shown recently [8], that in the isotropic and particle-hole symmetric case the long-range interaction favors the nematic instability, and if indeed the QBT point becomes unstable at low temperatures, then the rotational symmetry would break spontaneously. To substantiate this scenario and to understand to concomitant ordering, in the present work we therefore focus on the nematic interaction channel.

In order to establish the existence of a nematic QC point and to discuss its characteristics, in what follows we will suppress the long-range part of the Coulomb interaction. In the vicinity of the upper critical dimension, its inclusion is expected to only *quantitatively* improve our numerical predictions. Away from the upper critical dimension, however, the situation may, according to the scenario of the “fixed-point collision” [8], dramatically change, and we will briefly comment on this in the conclusions. The continuum quantum action, coupled to the fluctuating nematic order parameter, then is $S = \int d\tau d^d \vec{x} L$, with the Lagrangian density

$$L = L_\psi + L_{\psi\phi} + L_\phi, \quad (17)$$

and with the individual terms defined as

$$L_\psi = \psi^\dagger [\partial_\tau + \gamma_a d_a (-i\nabla)] \psi, \quad (18)$$

$$L_{\psi\phi} = g \phi_a \psi^\dagger \gamma_a \psi, \quad (19)$$

$$L_\phi = \frac{1}{4} T_{ij} (-c \partial_\tau^2 - \nabla^2 + r) T_{ji} + \lambda T_{ij} T_{jk} T_{ki} + \mathcal{O}(T^4). \quad (20)$$

ψ is the four-component Grassmann field, whereas ϕ_a is a real field. The summation over the repeated indices is now assumed, and $a = 1, \dots, 5$, and $i, j, k = 1, 2, 3$. γ_a are the five mutually anticommuting four-dimensional Dirac matrices introduced earlier.

The real, symmetric, traceless tensor field T_{ij} is defined as

$$T_{ij} = \phi_a \Lambda_{a,ij}, \quad (21)$$

where Λ_a are the five real, symmetric, three-dimensional Gell-Mann matrices. Their explicit form and important properties are discussed in Appendix A. Since the five spherical harmonics $d_a(\vec{p})$ transform as the components of the traceless symmetric tensor of rank 2 under rotations, the Lagrangian L will be invariant under rotations provided that the five components of the tensor T_{ij} , ϕ_a , $a = 1, \dots, 5$ do so as well.

At the level of the quantum mechanical averages

$$\langle \phi_a \rangle = \frac{-g}{r} \langle \psi^\dagger \gamma_a \psi \rangle, \quad (22)$$

and finding $\langle \phi_a \rangle \neq 0$ signals spontaneous breaking of the rotational symmetry. The tensor T_{ij} can be understood as the *nematic* order parameter, in analogy with liquid crystals, where the identical object describes the finite-temperature phase transition between the isotropic and anisotropic phases [24].

In the context of 2D metals, a nematic QC point describing the $\ell = 2$ Pomeranchuk instability of Fermi-liquid theory has been thoroughly investigated previously [29,30] and still commands attention [31], also due to its potential role in the phase diagram of certain high-temperature superconductors [32]. Nematic instabilities have also been predicted in 2D Fermi systems with QBT [2–4]. In two dimensions, however, the order parameter is odd under $\pi/2$ spatial rotation, which forbids a cubic term $\propto \text{Tr} T^3$ in the action [29]. By contrast, the 3D system defined by Eqs. (17)–(20) is an immediate generalization of the field theory describing the classical nematic transition in liquid crystals [24], which is recovered when the fermions are decoupled, i.e., in the limit $g \rightarrow 0$. The critical point we will find shortly therefore represents possibly the simplest quantum analog of this familiar classical nematic transition.

The above form of the Lagrangian L contains the minimal number of parameters, and the imaginary time, length, and the Grassmann and the real fields have been rescaled so the coefficients in front of the first and the second terms in L_ψ , and the second term in L_ϕ , are brought to unity. Besides the tuning parameter r , this still leaves the coefficient in the first term in L_ϕ , c , and the two interaction coupling constants: Yukawa coupling g and the cubic term self-interaction λ . These have the engineering dimensions

$$\dim[g] = \dim[\lambda] = \frac{6 - z - d}{2}, \quad (23)$$

whereas

$$\dim[c] = 2 - 2z. \quad (24)$$

Keeping the coefficients in L_ψ fixed demands the dynamical critical exponent to be $z = 2$ at the Gaussian fixed point $\lambda = g = 0$. One then finds that both couplings g and λ become relevant in the infrared *simultaneously* below $d = 4$. This observation allows one to formulate a perturbative approach to the problem of the infrared behavior as the expansion in the small parameter

$$\epsilon = 4 - d \quad (25)$$

and search for possible non-Gaussian critical points in the theory. The terms $\mathcal{O}(T^4)$ in L_ϕ have for this reason been omitted as irrelevant to the leading order in ϵ . The parameter c also is irrelevant at the Gaussian fixed point when $z = 2$. At the QC fixed point, however, we will find c to be shifted to a finite positive value, leading to nontrivial dynamical scaling of the order parameter (see Sec. V).

The rescaling procedure involves an apparent ambiguity, as one might equally well fix the coefficient c in front of the first term in L_ϕ , $\propto c(T_{ij} \partial_\tau^2 T_{ji})/4$, to unity, and let the coefficient, let us call it a , in front of the first term in L_ψ , $\propto a(\psi^\dagger \partial_\tau \psi)$,

to flow instead. This would dictate a different dynamical exponent, $z = 1$, at the Gaussian fixed point, reflecting the fact that the noninteracting system possesses two different characteristic time scales. In Appendix D we show that this alternative prescription leads to an equivalent RG flow and the *same* universal quantities at criticality. The QC point thus will be characterized by a single diverging time scale and a unique dynamical exponent. A similar ambiguity occurs in the effective order-parameter theory for the nematic instability in 2D metals, when the fermions have been integrated out, though its resolution differs from the present case [33].

We should also comment on yet another rotational invariant quadratic in T_{ij} , which is proportional to

$$\partial_i T_{ij} \partial_k T_{kj} \quad (26)$$

and that we have omitted in L_ϕ . It couples spatial rotations to internal rotations of the nematic order parameter and is thus possible only when the dimension p of the tensor T_{ij} ($i, j = 1, \dots, p$) is equal to the spatial dimension d (as is the case in our problem). We find that although of the same engineering dimension as the term we included at the noninteracting fixed point, this term develops a *negative* anomalous dimension to the leading order in interactions, and as such we expect it to become irrelevant at the interacting critical point (see Appendix C). One can analogously justify the common omission of this term in the studies of the classical isotropic-to-nematic transition in three dimensions.

IV. MEAN-FIELD THEORY

Before we present the solution of the problem in the vicinity of the upper critical dimension, let us consider the mean-field theory in which the fluctuations of the order-parameter field ϕ_a are neglected. This approximation can be justified by adding an additional ‘‘flavor’’ index to the fermions (e.g., by allowing more than one QBT point at the Fermi level) and taking the limit of large flavor number N [8]. The mean-field theory is solved by minimizing the total energy

$$E_{\text{MF}}(\phi_1, \dots, \phi_5) = \frac{r}{2} \phi_a \phi_a + 2 \int_0^\Lambda \frac{d\vec{p}}{(2\pi)^3} \varepsilon(\vec{p}), \quad (27)$$

where $\varepsilon(\vec{p})$ denote the lower-branch energy eigenvalues of the mean-field Hamiltonian $H_{\text{MF}}(\vec{p}) = p^2 \tilde{d}_a(\theta, \varphi) \gamma_a + g \phi_a \gamma_a$ in the presence of constant ϕ_a , viz.,

$$\varepsilon(p, \theta, \varphi) = -p^2 \sqrt{1 + 2\tilde{d}_a(\theta, \varphi) \frac{g\phi_a}{p^2} + \left(\frac{g\phi_a}{p^2}\right)^2}. \quad (28)$$

Λ is the UV momentum cutoff, $0 \leq |\vec{p}| \leq \Lambda$. For convenience, and without loss of generality, let us assume $g > 0$. The first term in Eq. (27) represents the energy cost of a finite ϕ_a . By contrast, the second term decreases with increasing order parameter, and thus involves the energy gain due to a (possible) ordering. It can be interpreted as the sum of the energies of the filled, doubly degenerate single-particle states in the ordered phase, with the Fermi level at the QBT. In the present model without the long-range Coulomb interaction and in $d = 3$ we expect the ordered state to be energetically favorable if the parameter g^2/r exceeds a certain strong-coupling threshold. This threshold, however, may decrease substantially upon the

inclusion of the long-range part of the Coulomb repulsion and might even vanish completely [8].

In the reference frame in which the tensor order parameter becomes diagonal,

$$(T_{ij}) = \begin{pmatrix} \phi_1 - \frac{\phi_5}{\sqrt{3}} & 0 & 0 \\ 0 & -\phi_1 - \frac{\phi_5}{\sqrt{3}} & 0 \\ 0 & 0 & 2\frac{\phi_5}{\sqrt{3}} \end{pmatrix}, \quad (29)$$

we can write $(\phi_a) = (\phi \sin \xi, 0, 0, 0, \phi \cos \xi)$ with $\phi := \sqrt{\phi_a \phi_a} \geq 0$. Shifting the parameter ξ by $\xi \mapsto \xi + 2\pi/3$ corresponds to a cyclic permutation of the x , y , and z axes. For example, the state $(\phi_a) = \phi(\sqrt{3}/2, 0, 0, 0, 1/2)$ for $\xi = \pi/3$ transforms into the state $(\phi_a) = \phi(0, 0, 0, 0, -1)$ for $\xi = \pi$ by permuting $(x, y, z) \mapsto (y, z, x)$. We may thus restrict the range of ξ to $0 \leq \xi < 2\pi/3$. Finding a finite $\phi \neq 0$ to be energetically favorable corresponds to a spontaneous breaking of the rotational symmetry. While for generic ξ no continuous part of the symmetry is left intact, for $\xi \equiv 0 \pmod{2\pi/3}$ or $\xi \equiv \pi/3 \pmod{2\pi/3}$ only two generators of the $O(3)$ are broken, with a residual $O(2)$ symmetry resulting. The corresponding *uniaxial* states $(\phi_a) = (0, 0, 0, 0, \pm\phi)$ (modulo rotations) are characterized by a single director, in analogy to the uniaxial nematic phase in liquid crystals [24].

The energy in the present basis reads as

$$E_{\text{MF}}(\phi, \xi) = \frac{r}{2} \phi^2 - 2(g\phi)^{5/2} \int_0^{\frac{\Lambda}{\sqrt{g\phi}}} dx \int \frac{d\Omega}{(2\pi)^3} \times x^2 \sqrt{x^4 + 2x^2(\tilde{d}_1 \sin \xi + \tilde{d}_5 \cos \xi) + 1}, \quad (30)$$

where we substituted $p/\sqrt{g\phi} \mapsto x$ and abbreviated the angular integration as $\int d\Omega = \int_0^\pi d\theta \sin \theta \int_0^{2\pi} d\varphi$. The integral becomes finite for $\Lambda/\sqrt{g\phi} \rightarrow \infty$ when we add a suitably written zero (corresponding to the parts in E_{MF} that are constant and quadratic in ϕ , respectively) as

$$0 = -\frac{4\pi}{(2\pi)^3} \left(\frac{2}{5} \Lambda^5 + \frac{4}{5} \Lambda g^2 \phi^2 \right) + 2(g\phi)^{5/2} \int_0^{\frac{\Lambda}{\sqrt{g\phi}}} dx \int \frac{d\Omega}{(2\pi)^3} \left(x^4 + \frac{2}{5} \right). \quad (31)$$

The mean-field energy then is (modulo irrelevant additive constants $\propto \Lambda^5$)

$$E_{\text{MF}}(\phi, \xi) = \frac{r'}{2} \phi^2 + t(\xi)(g\phi)^{5/2} + \mathcal{O}(\phi^3) \quad (32)$$

with $r' = r - \frac{8}{5} \frac{4\pi\Lambda}{(2\pi)^3} g^2$ the curvature at the origin and with the coefficient of the nonanalytic term $\propto \phi^{5/2}$ as

$$t(\xi) = 2 \int_0^\infty dx \int \frac{d\Omega}{(2\pi)^3} \left[x^4 + \frac{2}{5} - x^2 \sqrt{x^4 + 2x^2(\tilde{d}_1 \sin \xi + \tilde{d}_5 \cos \xi) + 1} \right] \simeq \frac{4\pi}{(2\pi)^3} \left[\frac{\pi}{8} + \frac{1}{2} \left(\frac{19}{30} - \frac{\ln 3}{8} - \frac{\pi}{8} \right) (1 - \cos 3\xi) \right]. \quad (33)$$

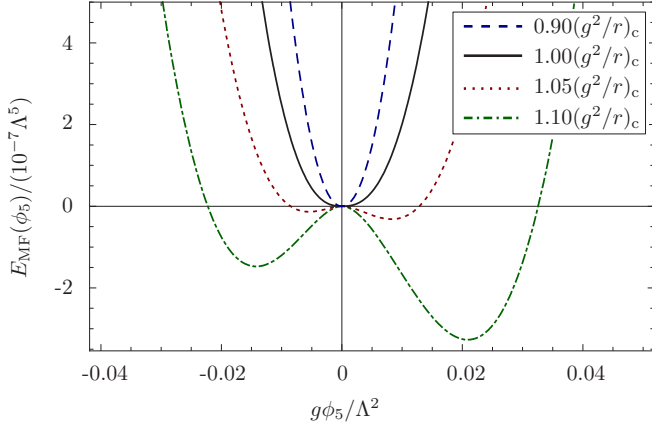


FIG. 1. (Color online) Mean-field energy $E_{\text{MF}}(\phi_5)$ for the uniaxial states $(\phi_a) = (0, 0, 0, 0, \phi_5)$ that preserve a residual $O(2)$ symmetry (i.e., $\xi \equiv 0 \pmod{2\pi/3}$ or $\xi \equiv \pi/3 \pmod{2\pi/3}$) for different values of the coupling g^2/r in the vicinity of the critical coupling $(g^2/r)_c$. The unique absolute minimum of the potential is at zero or positive $g\phi_5$, corresponding to the isotropic state and uniaxial nematic fully gapped state, respectively. The transition into the latter phase for overcritical coupling is continuous.

The second line of Eq. (33) approximates the numerical quadrature within an error range of $\lesssim 0.5\%$ for generic ξ and becomes exact for $\xi = 0$ and $\xi = \pi/3$. $t(\xi)$ is positive and bounded from below and above as $\frac{\pi}{8} \leq t(\xi) / \frac{4\pi}{(2\pi)^3} \leq \frac{19}{30} - \frac{\ln 3}{8}$. The QC point at the critical coupling

$$\left(\frac{g^2}{r}\right)_c = \frac{5(2\pi)^3}{84\pi\Lambda}, \quad (34)$$

when the curvature r' of $E_{\text{MF}}(\phi, \xi)$ at $\phi = 0$ changes sign, thus corresponds to a *continuous* phase transition—in contrast to the discontinuous (at least on the mean-field level) classical isotropic-to-nematic transition in liquid crystals [24]. A similar such unconventional continuous phase transition has recently been found in a model describing the spontaneous breaking of time-reversal symmetry in the pyrochlore iridates [34].

$t(\xi)$ attains its unique minimum at $\xi = 0$. When $g^2/r > (g^2/r)_c$ the transition is thus into the state with the order parameter $(\phi_a) = (0, 0, 0, 0, \phi)$, $\phi > 0$, which breaks the rotational $O(3)$ symmetry but leaves rotations about the z axis intact. The spectrum of fermions in this state has a full, anisotropic (θ -dependent) gap, with the minimal value at $\theta = \pi/2$ and $p^2 = g\phi/2$ of $\sqrt{3}g\phi/2$. The system appears as if under (dynamically generated) uniaxial strain [7,35], and, for the systems with the band structure equivalent to that of α -Sn or HgTe, represents a topological Mott insulator [8]. We depict the mean-field energy $E_{\text{MF}}(\phi_5)$ for the $O(2)$ -invariant states $(\phi_a) = (0, 0, 0, 0, \phi_5)$ for different values of the coupling g^2/r in Fig. 1, illustrating the continuous nature of the transition and the energetically favored minimum at $g\phi_5 > 0$ [36].

V. RG FLOW EQUATIONS

In order to show the existence of the nematic QC point beyond the mean-field theory we include next the effects of the bosonic fluctuations. To this end we perform the standard Wilson's renormalization group calculation, in which both the

order parameter and the fermionic fields with the momenta within the momentum shell $[\Lambda/b, \Lambda]$ and with all Matsubara frequencies are integrated out [37]. At the critical surface $r = 0$, to the leading order in the self-interaction λ and the Yukawa coupling g the result is the differential flow of the couplings:

$$\frac{dc}{d \ln b} = (2 - 2z - \eta_\phi)c + \frac{2}{5}g^2 + \frac{21}{4}\sqrt{c}\lambda^2, \quad (35)$$

$$\frac{dg}{d \ln b} = \frac{1}{2}(6 - d - z - \eta_\phi - 2\eta_\psi)g + \frac{6}{5}H(c)g^3, \quad (36)$$

$$\frac{d\lambda}{d \ln b} = \frac{1}{2}(6 - d - z - 3\eta_\phi)\lambda - \frac{27}{4}\frac{\lambda^3}{\sqrt{c}} - \frac{\sqrt{3}}{35}g^3. \quad (37)$$

Here we have rescaled the couplings as $g^2\Lambda^{d+z+\eta_\phi+2\eta_\psi-6}S_d/(2\pi)^d \mapsto g^2$ and $\lambda^2\Lambda^{d+z+3\eta_\phi-6}S_d/(2\pi)^d \mapsto \lambda^2$ with S_d the surface area of the $(d-1)$ sphere. The parameter c has been rescaled as $c\Lambda^{2z+\eta_\phi-2} \mapsto c$. The order parameter's and the fermion's anomalous dimensions, and the dynamical critical exponent, are to the leading order

$$\eta_\psi = \frac{4}{5}F(c)g^2, \quad (38)$$

$$\eta_\phi = \frac{44}{35}g^2 + \frac{21}{4}\frac{\lambda^2}{\sqrt{c}}, \quad (39)$$

$$z = 2 + \frac{5}{2}G(c)g^2 - \eta_\psi. \quad (40)$$

The functions $F(c)$, $G(c)$, and $H(c)$ are the result of the one-loop frequency integrals and are defined as

$$F(c) = \frac{8 + 9\sqrt{c} + 3c}{8(1 + \sqrt{c})^3}, \quad (41)$$

$$G(c) = \frac{\sqrt{c}}{(1 + \sqrt{c})^2}, \quad (42)$$

$$H(c) = \frac{4 + 3\sqrt{c}}{4(1 + \sqrt{c})^2}. \quad (43)$$

Small perturbations out of the critical surface are relevant in the sense of the RG and governed by the flow equation

$$\frac{dr}{d \ln b} = (2 - \eta_\phi)r - \frac{8}{5}g^2 - 21\frac{\lambda^2}{\sqrt{c}}\frac{1}{(1+r)^{3/2}}, \quad (44)$$

where we have rescaled $r\Lambda^{\eta_\phi-2} \mapsto r$.

Two comments on the computation of the RG flow equations are in order: First, we have chosen the anomalous dimensions η_ψ and η_ϕ and the dynamical exponent z so the coefficients in both terms in L_ψ as well as the momentum term in L_ϕ [i.e., $T_{ij}(-\nabla^2)T_{ji}/4$] remain unity after the mode elimination, which forces the remaining coefficient c in L_ϕ then to flow. However, while c is irrelevant at the Gaussian fixed point, its stable fixed-point value is shifted towards finite $c > 0$ when $g \neq 0$. At an interacting fixed point c thus scales as $c \propto \xi^{2z+\eta_\phi-2}$ relative to a characteristic (diverging) length scale $\xi \propto \omega^{-1/z}$. The scaling form of the inverse two-point function at the anticipated QC point then is

$$\langle \phi_a(\omega, \vec{p}) \phi_b(0, 0) \rangle^{-1} = p^{2-\eta_\phi} f\left(\frac{\omega}{p^z}\right) \delta_{ab} \quad (45)$$

with the scaling function f that has the asymptotic limits

$$f(x) \propto \begin{cases} 1 & \text{for } x \ll 1, \\ x^{(2-\eta_\phi)/z} & \text{for } x \gg 1. \end{cases} \quad (46)$$

The alternative scaling prescription that chooses the anomalous dimensions and the dynamical exponent such that the coefficients of both the momentum and frequency terms in L_ϕ remain fixed, and in turn allows a flowing parameter a in front of the frequency term in L_ψ , $a(\psi^\dagger \partial_\tau \psi)$, leads to the equivalent flow equations and same universal predictions at the interacting fixed point (see Appendix D).

Second, in order to arrive at Eqs. (35)–(44), we have kept the general counting of dimensions in the couplings but have performed the angular integrations directly in $d = 3$ spatial dimensions. For details we refer to Appendix C. In Appendix E we present the analogous derivation of the RG flow for the theory near $d = 4$ with nine-component order-parameter field ϕ_a and 16×16 gamma matrices γ_a , $a = 1, \dots, 9$.

The mean-field result from the previous section can be recovered by neglecting all bosonic fluctuations (e.g., by reintroducing the flavor number N and taking the limit of large N). The flow equation for the coupling g^2/r then becomes

$$\frac{d(g^2/r)}{\ln b} = (2-d)\frac{g^2}{r} + \frac{8}{5}\left(\frac{g^2}{r}\right)^2, \quad (47)$$

which in $d = 3$ has the zero exactly at the mean-field critical coupling $(g^2/r)_c = 5/8$, cf. Eq. (34) and the coupling rescalings below Eqs. (37) and (44).

To show that there exists a stable (quantum critical) fixed point of the equations also at $N = 1$ we introduce new variables:

$$u = \frac{\lambda}{c^{1/4}}, \quad v = \frac{g}{c^{1/12}}, \quad (48)$$

with c chosen such that it satisfies its own fixed-point equation:

$$0 = (2-2z)c + \left(\frac{2}{5} - \frac{44}{35}c\right)c^{1/6}v^2. \quad (49)$$

In terms of the new variables we can rewrite the flow equations as

$$\frac{du}{d \ln b} = \frac{1}{2}(\epsilon + 2 - z - 3\eta_\phi)u - \frac{27}{4}u^3 - \frac{\sqrt{3}}{35}v^3, \quad (50)$$

$$\frac{dv}{d \ln b} = \frac{1}{2}(\epsilon + 2 - z - \eta_\phi - 2\eta_\psi)v + \frac{6}{5}c^{1/6}H(c)v^3, \quad (51)$$

where we used Eq. (49) and also displayed the small parameter $\epsilon = 4 - d$.

After this change of variables, the stable fixed point is readily found to lie at $u = \mathcal{O}(\epsilon^{1/2})$, $v = \mathcal{O}(\epsilon^{1/2})$, and $c = \mathcal{O}(\epsilon^{6/5})$. Since $F(0) = 1$, $G(0) = 0$, and $H(0) = 1$, the fixed point features the critical exponents at leading order in ϵ ,

$$\eta_\psi = \mathcal{O}(\epsilon^{6/5}), \quad \eta_\phi = \epsilon + \mathcal{O}(\epsilon^{6/5}), \quad z = 2 + \mathcal{O}(\epsilon^{6/5}), \quad (52)$$

and it is located at the values of u and v that satisfy the equations:

$$\frac{21}{4}u^2 = \epsilon, \quad \frac{\sqrt{3}}{35}v^3 = u\left(-\epsilon - \frac{27}{4}u^2\right). \quad (53)$$

The last equation, in particular, implies that at the fixed point $\text{sgn}(v) = -\text{sgn}(u)$, whereas the first one leaves the sign of u undetermined. We find the following finite fixed-point values

$$u_\pm^* = \mp \frac{2}{\sqrt{21}}\sqrt{\epsilon}, \quad v_\pm^* = \pm 2\left(\frac{20}{3}\right)^{\frac{1}{3}}\left(\frac{1}{7}\right)^{\frac{1}{6}}\sqrt{\epsilon}. \quad (54)$$

As the partition function is invariant under the *simultaneous* sign change of g and λ , so are the flow equations. Thus, the two fixed points at (u_\pm^*, v_\pm^*) are physically equivalent. It is easy to check that this fixed point is indeed critical, i.e., with no other unstable directions except for the direction of the tuning parameter r . From the flow of r we find the exponent ν that governs the scaling of the correlation length $\xi \propto |\delta|^{-\nu}$, with δ denoting the deviation from the critical point, as

$$1/\nu = 2 + 5\epsilon + \mathcal{O}(\epsilon^{6/5}). \quad (55)$$

Notably, the correction to the mean-field exponent $1/\nu = 2$ is positive, in contrast to the QC points in Dirac fermion systems that are described by the $z = 1$ Gross-Neveu universality classes [21,38]. The reason for the difference in sign is the presence of the cubic term $\propto \text{Tr } T^3$ in the action, which renders the bosonic contribution to the flow equation of the tuning parameter r [last term in Eq. (44)] of opposite sign as compared to systems with quartic bosonic interactions. Likewise, in the field theory of the classical isotropic-to-nematic phase transition in liquid crystals which allows the cubic tensor invariant, the leading correction to $1/\nu$ is also positive [39].

We emphasize that our quantitative predictions for the critical exponents obtained near the upper critical dimension, although interesting in their own right, may not describe well real 3D systems in which long-range Coulomb interaction is important, such as α -Sn or HgTe. In these cases, a nematic gap might already open up at infinitesimal coupling [8]. Our result, however, at the very least shows that a QC fixed point *exists* near the upper critical dimension, substantiating the “fixed-point-collision” scenario, and it allows us to study the *qualitative* properties of the nematic instability. We therefore refrained from displaying the subleading terms $\propto \epsilon^{6/5}$ in Eqs. (52) and (55), which are straightforwardly computable from our one-loop flow equations, but do not, in our opinion, necessarily have direct relevance for the physics in $d = 3$.

We have plotted the leading-order RG flow in the u - v plane for $c = \mathcal{O}(\epsilon^{6/5})$ in Fig. 2, showing besides the unstable Gaussian (G) and stable fermionic (F) fixed points also the purely bosonic fixed point (B) at $v = 0$ and finite $u \neq 0$. B is unstable in the direction of v , in analogy to the bosonic Wilson-Fisher fixed point in Dirac fermion systems [21].

In the calculation with four-dimensional tensor order parameter we find that the bosonic fixed point B disappears, in full analogy to the $p = 4$ critical point in the field theory of the classical isotropic-to-nematic phase transition in liquid crystals [39]. In contrast, the fermionic fixed point (F in Fig. 2) survives for any dimension p of the tensor field, changing only its stability properties at larger values of p . Furthermore, our universal predictions for the anomalous dimensions η_ϕ and η_ψ as well as the critical exponents z and $1/\nu$ at the fermionic fixed point turn out to agree at leading order exactly with Eqs. (52) and (55), see Appendix E.

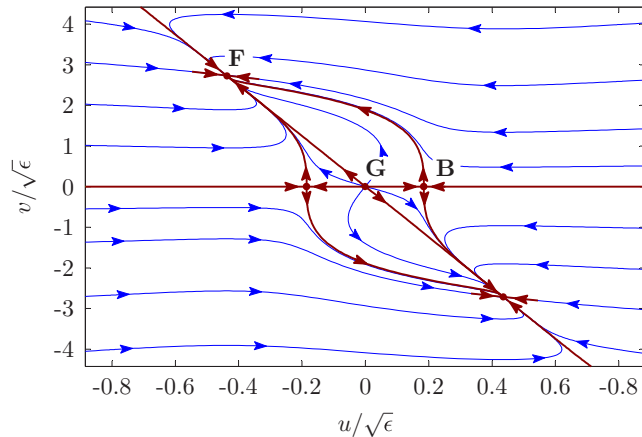


FIG. 2. (Color online) RG flow in the u - v plane for $r = 0$ and $c = \mathcal{O}(\epsilon^{6/5})$ to leading order in ϵ . Arrows point towards infrared. The purely bosonic fixed point (B) is unstable in direction of the Yukawa coupling v . The fermionic fixed point (F) is critical, with no other unstable directions except for the direction of the tuning parameter r . It governs the transition into an infrared phase that has fully gapped fermions and a spontaneously broken rotational symmetry.

VI. INTERPRETATION

At the mean-field level, the model features a continuous (quantum) phase transition, described by the large- N fixed point of the Gross-Neveu-Yukawa field theory. It therefore seems natural to associate the identified fixed point also for $N = 1$ with a continuous nematic quantum phase transition. One should note, however, that near the upper critical dimension and at small N the parameter c in L_ϕ becomes small at the fixed point, emphasizing the significance of purely bosonic fluctuations. The result of the mean-field theory may thus as well be overturned in the physical limit, and the possibility that at small N the nature of the transition differs from the mean-field picture cannot be excluded with certainty. We believe, nonetheless, that even in a scenario with a discontinuous quantum phase transition the above critical fixed point would still retain its physical significance: such a situation arises, for example, in the related classical Ginzburg-Landau-Wilson theory for the (presumably discontinuous) thermal isotropic-to-nematic transition in liquid crystals, which also exhibits a critical fixed point in the related $\epsilon = 6 - d$ expansion [39]. A plausible interpretation of the latter is that it describes the disappearance of the energy barrier between the high- and low-temperature phases and the ultimate instability of the metastable symmetric phase.

An interesting feature of the identified fixed point is worth pointing out. In the reference frame where the nematic tensor would become diagonal [Eq. (29)], the bosonic part of the Lagrangian for uniform order parameter ($\phi_a = (\phi \sin \xi, 0, 0, 0, \phi \cos \xi)$, $\phi > 0$), becomes

$$L_\phi = \frac{r}{2}\phi^2 + \frac{2\lambda}{\sqrt{3}}\cos(3\xi)\phi^3 + b\phi^4 + \mathcal{O}(\phi^5), \quad (56)$$

where we have displayed the unique symmetry-allowed quartic term as well. At intermediate steps of the RG the Lagrangian is analytic in ϕ , and the nonanalytic term $\propto \phi^{5/2}$ will only emerge in the deep infrared, when all modes are integrated out. During

this process it may in general receive contributions from the flow of all higher-order terms. If we focus for simplicity only on the leading cubic and quartic invariants and consider (without loss of generality) the fixed point at $\lambda < 0$, we find that the effective quantum potential at the fixed point is minimized for $\xi = 0$. If this remains true up to the infrared, when the $\phi^{5/2}$ term in L_ϕ emerges, it indicates that the interacting ground state for strong coupling has (also for small N) the uniaxial form with $\phi_5 > 0$ and $\phi_1 = 0$. The fate of fermions in this state depends crucially then on the sign of the remaining Yukawa coupling g . If $g > 0$, then the combination $g\phi_5 > 0$, and we recover the mean-field ground state with the spectrum of fermions having the full, anisotropic gap (cf. Sec. IV). If, on the other hand, $g < 0$ and $g\phi_5 < 0$, the spectrum has two gapless points in the vicinity of which the energy dispersion becomes linear [8].

We see, however, that the leading term in the flow equation for λ is $-g^3$, so a negative self-interaction λ is generated only by a *positive* Yukawa coupling g . This is reflected in the fixed-point location, at which the signs of the two couplings are inevitably opposite. Incidentally, this feature is also responsible for the stability of the fixed point. Also, even if we start the RG flow at microscopic couplings λ and g of the same sign, we always flow to a regime in which $\lambda g < 0$, at least in the vicinity of the critical surface (see Fig. 2). We thus find that the consistent theory in the infrared has the fermions fully gapped in the broken symmetry phase, in agreement with the mean-field result.

VII. CONCLUSIONS

In sum, we constructed the field theory of the fermions with the chemical potential at the point of quadratic band touching in three spatial dimensions coupled to the second-rank tensorial nematic order parameter. We argued that this field theory has an upper critical dimension of four and that it possesses a perturbatively accessible quantum critical point in the vicinity of four dimensions. The critical point governs the (presumably continuous) transition between the semimetal to the fully, but anisotropically gapped, Mott insulator. The existence of the critical point in the theory supports the scenario of the “fixed-point collision” [8], according to which the Fermi system with QBT in the presence of the long-range tail of Coulomb interaction, which we have here suppressed, features a lower critical dimension d_{low} with $2 < d_{\text{low}} < 4$. At d_{low} the nematic QC point and the Abrikosov’s NFL fixed point collide and then disappear from the real space of physical couplings, leaving behind the runaway flow. The ground-state physics of the 3D systems such as clean α -Sn or HgTe crucially depends on whether d_{low} is above or below $d = 3$. The one-loop analysis points to d_{low} slightly above three, which would make the QBT point unstable towards the nematic insulator even in the weak-coupling limit [8]. If, on the other hand, the true value of d_{low} would turn out to be below 3 and both the Abrikosov’s NFL as well as the QC fixed points persist all the way down to the physical dimension, the weakly interacting systems are governed by the attractive NFL fixed point and should exhibit anomalous power laws in several observables [7]. If d_{low} is below but not too far from $d = 3$, however, and the nematic QC point is, consequently, located at not too large a coupling, one

could still speculate on situations, e.g., in *uniformly* strained systems or in cold-atom quantum simulators, in which the interactions may be tuned through the nematic QC point. In any case, it would obviously be desirable to gain a firmer theoretical control over the true value of d_{low} . This work is underway [40].

ACKNOWLEDGMENTS

We thank F. Assaad, B. Dóra, H. Gies, L. Golubović, Y. Meurice, W. Metzner, A. Rosch, B. Roy, B. Skinner, and especially Oskar Vafek for discussions on this and related subjects, and we are grateful to M. Vojta for pointing us to Ref. [33] and the problem of multiple dynamic scaling. The support from the Deutsche Forschungsgemeinschaft under JA 2306/1-1 and the NSERC of Canada is acknowledged.

APPENDIX A: GENERALIZED REAL GELL-MANN MATRICES

For completeness, let us review the construction of the generalized Gell-Mann matrices in d dimensions [the generators

of $SU(d)$] [41]. They can be classified into three groups. The first group is given by the real, diagonal, and traceless matrices

$$\hat{w}_l = -\sqrt{\frac{2}{l(l+1)}} \sum_{j=1}^l (|j\rangle\langle j| - |l+1\rangle\langle l+1|), \quad (\text{A1})$$

where $1 \leq l \leq d-1$ and $|1\rangle, \dots, |d\rangle$ denote the (standard) orthonormal basis vectors in \mathbb{R}^d , $\langle i|j\rangle = \delta_{ij}$. The second group are $d(d-1)/2$ real symmetric matrices that have nonvanishing elements only on the off-diagonal, namely the matrices \hat{u}_{jk} with ones in the jk -th and kj -th entries and zero otherwise,

$$\hat{u}_{jk} = |j\rangle\langle k| + |k\rangle\langle j|, \quad \text{where } 1 \leq j < k \leq d. \quad (\text{A2})$$

The third group are $d(d-1)/2$ imaginary matrices which can be constructed similarly to \hat{u}_{jk} . However, for the purposes of the present work we only need the *real* Gell-Mann matrices of the first and second groups.

In $d=2$, this construction gives $\hat{w}_1 = -\sigma_3$ and $\hat{u}_{12} = \sigma_1$. In $d=3$, we recover the standard (modulo name and sign conventions) 3×3 real Gell-Mann matrices:

$$\begin{aligned} \Lambda_1 = -\hat{w}_1 &= \begin{pmatrix} 1 & 0 & 0 \\ 0 & -1 & 0 \\ 0 & 0 & 0 \end{pmatrix}, & \Lambda_2 = \hat{u}_{12} &= \begin{pmatrix} 0 & 1 & 0 \\ 1 & 0 & 0 \\ 0 & 0 & 0 \end{pmatrix}, & \Lambda_3 = \hat{u}_{13} &= \begin{pmatrix} 0 & 0 & 1 \\ 0 & 0 & 0 \\ 1 & 0 & 0 \end{pmatrix}, \\ \Lambda_4 = \hat{u}_{23} &= \begin{pmatrix} 0 & 0 & 0 \\ 0 & 0 & 1 \\ 0 & 1 & 0 \end{pmatrix}, & \Lambda_5 = \hat{w}_2 &= \frac{1}{\sqrt{3}} \begin{pmatrix} -1 & 0 & 0 \\ 0 & -1 & 0 \\ 0 & 0 & 2 \end{pmatrix}. \end{aligned} \quad (\text{A3})$$

In $d=4$, we find

$$\begin{aligned} \Lambda_1 &= \begin{pmatrix} 1 & 0 & 0 & 0 \\ 0 & -1 & 0 & 0 \\ 0 & 0 & 0 & 0 \\ 0 & 0 & 0 & 0 \end{pmatrix}, & \Lambda_2 &= \begin{pmatrix} 0 & 1 & 0 & 0 \\ 1 & 0 & 0 & 0 \\ 0 & 0 & 0 & 0 \\ 0 & 0 & 0 & 0 \end{pmatrix}, & \Lambda_3 &= \begin{pmatrix} 0 & 0 & 1 & 0 \\ 0 & 0 & 0 & 0 \\ 1 & 0 & 0 & 0 \\ 0 & 0 & 0 & 0 \end{pmatrix}, \\ \Lambda_4 &= \begin{pmatrix} 0 & 0 & 0 & 0 \\ 0 & 0 & 1 & 0 \\ 0 & 1 & 0 & 0 \\ 0 & 0 & 0 & 0 \end{pmatrix}, & \Lambda_5 &= \frac{1}{\sqrt{3}} \begin{pmatrix} -1 & 0 & 0 & 0 \\ 0 & -1 & 0 & 0 \\ 0 & 0 & 2 & 0 \\ 0 & 0 & 0 & 0 \end{pmatrix}, & \Lambda_6 &= \begin{pmatrix} 0 & 0 & 0 & 1 \\ 0 & 0 & 0 & 0 \\ 0 & 0 & 0 & 0 \\ 1 & 0 & 0 & 0 \end{pmatrix}, \\ \Lambda_7 &= \begin{pmatrix} 0 & 0 & 0 & 0 \\ 0 & 0 & 0 & 1 \\ 0 & 0 & 0 & 0 \\ 0 & 1 & 0 & 0 \end{pmatrix}, & \Lambda_8 &= \begin{pmatrix} 0 & 0 & 0 & 0 \\ 0 & 0 & 0 & 0 \\ 0 & 0 & 0 & 1 \\ 0 & 0 & 1 & 0 \end{pmatrix}, & \Lambda_9 &= \frac{1}{\sqrt{6}} \begin{pmatrix} -1 & 0 & 0 & 0 \\ 0 & -1 & 0 & 0 \\ 0 & 0 & -1 & 0 \\ 0 & 0 & 0 & 3 \end{pmatrix}. \end{aligned} \quad (\text{A4})$$

In general dimension d , the $(d^2-d)/2 + (d-1)$ off-diagonal and diagonal, respectively, real matrices Λ_a form an orthogonal set:

$$\text{Tr}(\Lambda_a \Lambda_b) = 2\delta_{ab}, \quad (\text{A5})$$

and, together with the unit matrix, they form a basis in the space of real symmetric d -dimensional matrices. We therefore can write the matrix element of any symmetric matrix M as

$$M_{ij} = \frac{1}{d} \delta_{ij} M_{kk} + \frac{1}{2} M_{lm} \Lambda_{a,ml} \Lambda_{a,ij} \quad (\text{A6})$$

or, equivalently, as

$$\frac{1}{2} (\delta_{li} \delta_{mj} + \delta_{lj} \delta_{mi}) M_{lm} = \left(\frac{1}{d} \delta_{ij} \delta_{lm} + \frac{1}{2} \Lambda_{a,ml} \Lambda_{a,ij} \right) M_{lm}. \quad (\text{A7})$$

From here we deduce an important relation:

$$\Lambda_{a,ml} \Lambda_{a,ij} = \delta_{li} \delta_{mj} + \delta_{lj} \delta_{mi} - \frac{2}{d} \delta_{ij} \delta_{lm}, \quad (\text{A8})$$

which we use in the computation of the RG flow equations.

APPENDIX B: QBT HAMILTONIAN IN d DIMENSIONS

We can construct the general QBT Hamiltonian $H = G_{ij} p_i p_j$ in d dimensions with the help of $(d^2 - d)/2 + (d - 1) = (d + 2)(d - 1)/2$ gamma matrices γ_a . They have dimension $d_\gamma = 2^{\lfloor (d+2)(d-1)/4 \rfloor}$ with $\lfloor \cdot \rfloor$ denoting the floor function. The relationship between the G_{ij} and the gamma matrices γ_a , $a = 1, \dots, (d + 2)(d - 1)/2$ are given by the real and symmetric (generalized) $d \times d$ Gell-Mann matrices Λ_a as

$$G_{ij} = \sqrt{\frac{d}{2(d-1)}} \Lambda_{a,ij} \gamma_a. \quad (\text{B1})$$

Together with the Clifford algebra $\{\gamma_a, \gamma_b\} = 2\delta_{ab}$ and Eq. (A8), this immediately gives $H^2 = p^4$, as expected. In any dimension, we can thus write the Hamiltonian in the form

$$H = d_a(\vec{p}) \gamma_a, \quad a = 1, \dots, \frac{1}{2}(d + 2)(d - 1), \quad (\text{B2})$$

with

$$d_a(\vec{p}) = p^2 \tilde{d}_a(\Omega) = \sqrt{\frac{d}{2(d-1)}} p_i \Lambda_{a,ij} p_j. \quad (\text{B3})$$

This defines the real hyperspherical harmonics $\tilde{d}_a(\Omega)$ for angular momentum of two in general dimension, with Ω denoting the spherical angles on the $(d - 1)$ sphere in \vec{p} space.

APPENDIX C: COMPUTATION OF RG FLOW EQUATIONS

Let us provide some details on the computation of the RG flow equations (35)–(40). In the perturbative expansion, after integrating out the high-energy modes with momenta in the thin shell $[\Lambda/b, \Lambda]$, we arrive at the effective action for the low-energy modes:

$$\begin{aligned} S_{<} = & \int_0^{\Lambda/b} \frac{d\vec{k}}{(2\pi)^d} \int_{-\infty}^{\infty} \frac{d\omega}{2\pi} \left\{ \psi^\dagger [b^{\eta_1} i\omega + b^{\eta_\psi} d_a(\vec{k}) \gamma_a] \psi \right. \\ & + \frac{1}{2} \phi_a [(c + \delta c)\omega^2 + b^{\eta_\phi} k^2 + (r + \delta r)] \phi_a \\ & + \left. (\beta + \delta\beta) k_i k_j \Lambda_{a,il} \Lambda_{b,lj} \phi_a \phi_b \right\} \\ & + \int_0^{\Lambda/b} \frac{d\vec{k}_1 d\vec{k}_2}{(2\pi)^{2d}} \int_{-\infty}^{\infty} \frac{d\omega_1 d\omega_2}{(2\pi)^2} [(g + \delta g) (\phi_a \psi^\dagger \gamma_a \psi) \\ & + (\lambda + \delta\lambda) \Lambda_{a,ij} \Lambda_{b,jl} \Lambda_{c,li} (\phi_a \phi_b \phi_c)], \quad (\text{C1}) \end{aligned}$$

where we have included the second symmetry allowed, quadratic, momentum-dependent term $\propto \beta k_i k_j T_{il} T_{lj}$ [third line in Eq. (C1)] for generality. The anomalous dimensions η_1 , η_ψ , and η_ϕ and the explicit renormalizations δc , δr , $\delta\beta$, δg , and $\delta\lambda$ are determined by evaluating the corresponding one-loop diagrams, as depicted in Fig. 3. η_1 and η_ψ are given by the fermion-boson loop in Fig. 3(a), expanded to first order in external frequency ω and second order in external momentum k , respectively. η_ϕ has two contributions, given by the diagrams in Figs. 3(b) and 3(c), when expanded to second order in external momentum. When alternatively expanded in frequency, these diagrams explicitly renormalize the frequency term $\propto c\omega^2 \phi_a^2$. The constant parts of the diagrams determine the shift of the tuning parameter r . At the upper critical dimension the coefficients of the diagrams become universal

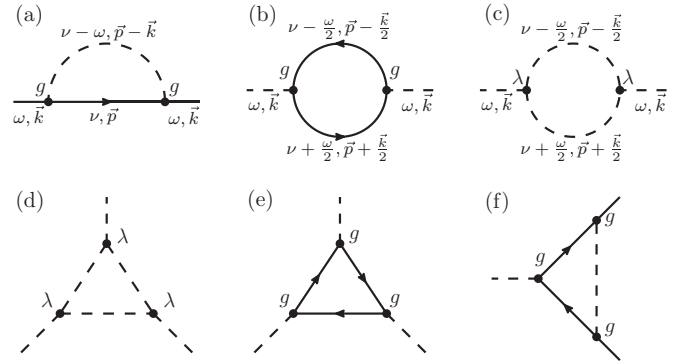


FIG. 3. Diagrams that contribute to the flow equations. Solid lines represent fermions and dashed lines represent bosons. Top: Contributions to (a) η_1 , η_ψ ; (b) η_ϕ , r , β ; and (c) η_ϕ , r . At finite external momenta \vec{k} and frequencies ω the diagrams are evaluated using the momentum and frequency routings as displayed, with loop momentum $|\vec{p}| \in [\Lambda/b, \Lambda]$ and frequency $\nu \in (-\infty, \infty)$. Bottom: Contributions to (d), (e) $d\lambda/d \ln b$, and (f) $dg/d \ln b$.

(see Appendix E). Here we will perform the angular integrations directly in $d = 3$ spatial dimensions. The diagrams may then receive (slight) regularization dependencies. To be explicit, we distribute finite external momentum and frequency in the fermion-boson loop in Fig. 3(a) such that the fermion loop momentum is on-shell, $|\vec{p}| \in [\Lambda/b, \Lambda]$, while we choose a symmetric momentum and frequency distribution in the fermion-fermion and the boson-boson loops in Figs. 3(b) and 3(c).

One further comment on the bosonic contribution to η_ϕ [Fig. 3(c)] should be made: We note that the diagram is invariant under the “pseudorelativistic” rotation $(\sqrt{c}\omega, \vec{k})_\mu \mapsto O_{\mu\nu}(\sqrt{c}\omega, \vec{k})_\nu$ with $(d + 1)$ -dimensional rotation matrix $O^T O = \mathbb{1}$, $\mu, \nu = 0, \dots, d$. In order to compute the contribution to η_ϕ one may therefore expand the diagram either in external frequency $c\omega^2$ or in external momentum k^2 , and both prescriptions should give the same result due to the “pseudorelativistic” invariance of the diagram. Put differently, in $dc/d \ln b$, the two contributions from η_ϕ and δc from this diagram should cancel. The invariance, however, is broken by our regularization scheme, in which we integrate out all frequencies at once, rendering the coefficients of the $c\omega^2$ term and the k^2 term different. It is therefore *a priori* not clear which one to choose as the one giving the contribution to η_ϕ . To resolve this issue we recompute the diagram Fig. 3(c) using a “pseudorelativistic” regularization with loop momentum and frequency $\Lambda/b \leq \sqrt{c\nu^2 + p^2} \leq \Lambda$, which gives the same contribution independent of whether one expands in $c\omega^2$ or k^2 . We find that the value obtained in this scheme is in fact exactly the same as the one obtained by expanding the diagram in $c\omega^2$ in our standard scheme, so we thus use this value as the bosonic contribution to η_ϕ .

The boson- and fermion-loop diagrams in Figs. 3(d) and 3(e), respectively, renormalize the bosonic self-interaction λ . In order to evaluate these diagrams, we continually make use of the identities in Eqs. (A8) and (B3) derived above. For instance, for the evaluation of the fermion loop in Fig. 3(e) we need the following angular integral over the $(d - 1)$ sphere in

\vec{p} space:

$$\begin{aligned} & \int d\Omega d_a(\vec{p})d_b(\vec{p})d_c(\vec{p}) \\ &= \left(\frac{d}{2(d-1)}\right)^{3/2} \int d\Omega p_i p_j p_k p_l p_m p_n \Lambda_{a,ij} \Lambda_{b,kl} \Lambda_{c,mn} \\ &= \sqrt{\frac{d}{2(d-1)}} \frac{4S_d}{(d-1)(d+2)(d+4)} \text{Tr}(\Lambda_a \Lambda_b \Lambda_c) p^6, \end{aligned} \quad (\text{C2})$$

where $S_d = 2\pi^{d/2}/\Gamma(d/2)$ is the surface area of the $(d-1)$ sphere and Ω again denotes the spherical angles on the sphere. The evaluation of the triangle diagram in Fig. 3(f), which renormalizes the Yukawa vertex g , is straightforward when making use of the orthogonality of the real spherical harmonics

$$\int d\Omega d_a(\vec{p})d_b(\vec{p}) = \frac{2S_d}{(d+2)(d-1)} p^4 \delta_{ab}. \quad (\text{C3})$$

In order to bring the cutoff in $S_<$ back to Λ we shift the momenta $b\vec{k} \mapsto \vec{k}$ and frequencies $b^z \omega \mapsto \omega$ with suitable dynamical exponent z . The coefficients of the momentum terms $\propto k^2$ in the fermionic and bosonic propagators in the first and second lines of Eq. (C1), respectively, can be fixed to 1 if we renormalize the fields as

$$b^{-(2+d+z-\eta_\psi)/2} \psi \mapsto \psi, \quad b^{-(2+d+z-\eta_\phi)/2} \phi \mapsto \phi. \quad (\text{C4})$$

However, then only one of the frequency terms can be fixed. We choose the fermionic term $\propto i\omega$, which is done by setting

$$z = 2 + \eta_1 - \eta_\psi. \quad (\text{C5})$$

At the noninteracting fixed point we thus have $z = 2$. The low-energy action $S_<$ is hence brought back into the same form as before integrating out the momentum shell if the couplings are renormalized as

$$\frac{dc}{d \ln b} = (2 - 2z - \eta_\phi)c + \frac{\partial \delta c}{\partial \ln b}, \quad (\text{C6})$$

$$\frac{dg}{d \ln b} = \frac{1}{2}(6 - d - z - \eta_\phi - 2\eta_\psi)g + \frac{\partial \delta g}{\partial \ln b}, \quad (\text{C7})$$

$$\frac{d\lambda}{d \ln b} = \frac{1}{2}(6 - d - z - 3\eta_\phi)\lambda + \frac{\partial \delta \lambda}{\partial \ln b}, \quad (\text{C8})$$

$$\frac{dr}{d \ln b} = (2 - \eta_\phi)r + \frac{\partial \delta r}{\partial \ln b}. \quad (\text{C9})$$

If we rescale the parameters as $c\Lambda^{2z+\eta_\phi-2} \mapsto c$, $g^2\Lambda^{d+z+\eta_\phi+2\eta_\psi-6}S_d/(2\pi)^d \mapsto g^2$, $\lambda^2\Lambda^{d+z+3\eta_\phi-6}S_d/(2\pi)^d \mapsto \lambda^2$, and $r\Lambda^{\eta_\phi-2} \mapsto r$, the explicit evaluation of the diagrams leads to Eqs. (35)–(44) in the main text.

Let us comment on the β term proportional to

$$k_i k_j \Lambda_{a,il} \Lambda_{b,lj} \phi_a \phi_b = k_i k_j T_{il} T_{lj}, \quad (\text{C10})$$

which couples the internal rotations of the tensor T to the spatial rotations. Evaluating the particle-hole diagram in Fig. 3(b) for zero external frequency involves the

integral

$$\begin{aligned} I_{ab}(\vec{k}) &= \int_{\Lambda/b}^{\Lambda} \frac{d\vec{p}}{(2\pi)^d} \int_{-\infty}^{\infty} \frac{dv}{2\pi} \\ &\times \text{Tr} \left[\gamma_a \frac{iv + d_c(\vec{p} + \vec{k})\gamma_c}{v^2 + (\vec{p} + \vec{k})^4} \gamma_b \frac{iv + d_e(\vec{p})\gamma_e}{v^2 + p^4} \right] \\ &= \frac{S_3}{(2\pi)^3} \left[-\frac{8}{5} \delta_{ab} \Lambda^2 + \frac{44}{35} k^2 \delta_{ab} - \frac{27}{70} k_i k_j \Lambda_{a,il} \Lambda_{b,lj} \right] \\ &\times \Lambda^{d-4} \ln b + \mathcal{O}(k^4), \end{aligned} \quad (\text{C11})$$

where in the last line we have for explicitness evaluated the angular integral in $d = 3$. We note that the contribution to the bosonic propagator $\propto k^2 \delta_{ab}$ [second term in Eq. (C11)] is larger than the contribution to the β term $\propto (\Lambda_a \vec{k})(\Lambda_b \vec{k})$ (third term). The anomalous dimension of the latter thus becomes *negative* and β is irrelevant in the sense of the RG. This justifies its omission in L_ϕ , as anticipated in Sec. III. Another way to view this is to regard β as a coupling which flows according to

$$\frac{d\beta}{d \ln b} = -\frac{44}{35} g^2 \beta - \frac{27}{140} g^2, \quad (\text{C12})$$

which indeed has a stable fixed point at $\beta = -27/176$. We note that the action is bounded from below when

$$\frac{\delta^2 S}{\delta \phi^a \delta \phi^b} > 0 \Leftrightarrow \frac{1}{2} + \frac{4}{3} \beta > 0, \quad (\text{C13})$$

and a negative fixed-point value for β is still consistent with stability.

APPENDIX D: ALTERNATIVE DYNAMICAL SCALING

We now show that the alternative dynamical scaling scheme in which we fix the coefficient c in front of the frequency term in L_ϕ and in turn allow for a flowing parameter a in front of the fermionic frequency term leads to the equivalent flow equations and the same universal observables at criticality. After integrating out the high-energy modes the low-energy effective action can be written as

$$\begin{aligned} S_< &= \int_0^{\Lambda/b} \frac{d\vec{k}}{(2\pi)^d} \int_{-\infty}^{\infty} \frac{d\omega}{2\pi} \left\{ \psi^\dagger [(a + \delta a)i\omega + b^{\eta_\psi} d_a(\vec{k})\gamma_a] \psi \right. \\ &+ \frac{1}{2} \phi_a [b^{\eta_2} \omega^2 + b^{\eta_\phi} k^2 + (r + \delta r)] \phi_a \\ &+ (\beta + \delta \beta) k_i k_j \Lambda_{a,il} \Lambda_{b,lj} \phi_a \phi_b \left. \right\} \\ &+ \int_0^{\Lambda/b} \frac{d\vec{k}_1 d\vec{k}_2}{(2\pi)^{2d}} \int_{-\infty}^{\infty} \frac{d\omega_1 d\omega_2}{(2\pi)^2} [(g + \delta g)(\phi_a \psi^\dagger \gamma_a \psi) \\ &+ (\lambda + \delta \lambda) \Lambda_{a,ij} \Lambda_{b,jl} \Lambda_{c,li} (\phi_a \phi_b \phi_c)], \end{aligned} \quad (\text{D1})$$

which is equivalent to Eq. (C1) upon identification

$$\eta_1 = \frac{1}{a} \frac{\partial \delta a}{\partial \ln b}, \quad \eta_2 = \frac{1}{c} \frac{\partial \delta c}{\partial \ln b}, \quad (\text{D2})$$

and $c = 1/a^2$. Note that although ω and k now have the same units, the engineering dimensions of g and λ still retain their above form, Eq. (23), albeit with a different dynamical exponent at the Gaussian fixed point. The engineering dimension

of the parameter a is

$$\dim[a] = 2 - z. \quad (\text{D3})$$

After the RG step $bk \mapsto k$, $b^2\omega \mapsto \omega$ and renormalizations of the fields as in Eq. (C4), both the momentum term and the frequency term of the bosonic field in $S_<$ can be brought back into the form of the initial action if we choose

$$z = \frac{1}{2}(2 + \eta_2 - \eta_\phi), \quad (\text{D4})$$

and thus $z = 1$ in the noninteracting limit. This is in contrast to Eq. (C5), reflecting the ambiguity of the dynamical scaling at the Gaussian fixed point. The β functions then become

$$\frac{da}{d \ln b} = (2 - z - \eta_\psi)a + \frac{5}{2}G(a^{-2})g^2, \quad (\text{D5})$$

$$\frac{dg}{d \ln b} = \frac{1}{2}(6 - d - z - \eta_\phi - 2\eta_\psi)g + \frac{6}{5}H(a^{-2})\frac{g^3}{a}, \quad (\text{D6})$$

$$\frac{d\lambda}{d \ln b} = \frac{1}{2}(6 - d - z - 3\eta_\phi)\lambda - \frac{27}{4}\lambda^3 - \frac{\sqrt{3}}{35}\frac{g^3}{a}, \quad (\text{D7})$$

with the anomalous dimensions

$$\eta_\psi = \frac{4}{5}F(a^{-2})\frac{g^2}{a}, \quad (\text{D8})$$

$$\eta_\phi = \frac{44}{35}\frac{g^2}{a} + \frac{21}{4}\lambda^2, \quad (\text{D9})$$

$$\eta_2 = \frac{2}{5}ag^2 + \frac{21}{4}\lambda^2, \quad (\text{D10})$$

and where we have rescaled g and λ as displayed below Eq. (37) in the main text and $\Lambda^{z+\eta_\psi-2}a \mapsto a$. The functions F , G , and H are also precisely the ones given in Eqs. (41)–(43) in the main text.

Starting the RG flow on the critical surface $r = 0$ in the vicinity of the Gaussian fixed point, $\lambda \simeq 0$, $g \simeq 0$, we have initially $z \simeq 1$, which renders the parameter a relevant in the sense of the RG. Together with a , however, z increases towards the infrared and the flow of a will eventually stop when the dynamical exponent satisfies

$$z = 2 + \eta_\psi - \frac{5}{2}G(a^{-2})\frac{g^2}{a}. \quad (\text{D11})$$

Equating Eqs. (D4) and (D11) determines the value of a at the interacting fixed point:

$$\left(2 - 2z - \frac{44}{35}\frac{g^2}{a}\right)\frac{1}{a^2} + \frac{2}{5}\frac{g^2}{a} = 0. \quad (\text{D12})$$

Upon rescaling $g^2/a \mapsto g^2$ and $\lambda^2/a \mapsto \lambda$ the Eq. (D12) becomes exactly the fixed-point equation for c [Eq. (35)] when $c = 1/a^2$. With this identification, the flow equations for g and λ as well as the anomalous dimensions and the dynamical exponent at the fixed point have precisely the same form as in the main text, cf. Eqs. (36)–(40) with Eqs. (D6)–(D11). The alternative dynamical scaling scheme therefore leads to the same fixed-point structure and universal critical exponents. The ambiguity in the dynamical scaling is thus resolved at the QC point, which is determined by the unique dynamical critical exponent

$$z = 2 + \mathcal{O}(\epsilon^{6/5}). \quad (\text{D13})$$

APPENDIX E: FLOW EQUATIONS FOR FOUR-DIMENSIONAL TENSOR FIELD

We finally discuss the flow equations and fixed-point structure when evaluating the angular integral directly at the upper critical dimension $d = 4$ with the nine 16×16 gamma matrices γ_a , the 16-component Dirac fermion ψ , and the four-dimensional tensor field T_{ij} , $i, j = 1, \dots, 4$ with its irreducible components ϕ_a , $a = 1, \dots, 9$. The computation of the one-loop diagrams in Fig. 3 now gives

$$\frac{dc}{d \ln b} = (2 - 2z - \eta_\phi)c + \frac{16}{9}g^2 + 9\sqrt{c}\lambda^2, \quad (\text{E1})$$

$$\frac{dg}{d \ln b} = \frac{1}{2}(6 - d - z - \eta_\phi - 2\eta_\psi)g + \frac{28}{9}\tilde{H}(c)g^3, \quad (\text{E2})$$

$$\frac{d\lambda}{d \ln b} = \frac{1}{2}(6 - d - z - 3\eta_\phi)\lambda + \frac{27}{2}\frac{\lambda^3}{\sqrt{c}} - \frac{1}{9}\sqrt{\frac{2}{3}}g^3, \quad (\text{E3})$$

with the anomalous dimensions

$$\eta_\psi = \frac{7}{6}F(c)g^2, \quad (\text{E4})$$

$$\eta_\phi = \frac{49}{9}g^2 + 9\frac{\lambda^2}{\sqrt{c}}, \quad (\text{E5})$$

$$z = 2 + \frac{9}{2}G(c)g^2 - \eta_\psi. \quad (\text{E6})$$

$F(c)$ and $G(c)$ are given in Eqs. (41)–(42) in the main text and

$$\tilde{H}(c) = \frac{8 + 7\sqrt{c}}{8(1 + \sqrt{c})^2}. \quad (\text{E7})$$

The flow of the tuning parameter is

$$\frac{dr}{d \ln b} = (2 - \eta_\phi)r - \frac{64}{9}g^2 - 36\frac{\lambda^2}{\sqrt{c}}\frac{1}{(1+r)^{3/2}}. \quad (\text{E8})$$

The only qualitative and universal difference to the computation in $d = 3$ is the sign of the λ^3 term in $d\lambda/d \ln b$, which eliminates the (unstable) purely bosonic fixed point (B in Fig. 2) at $g = 0$. This is in full analogy to the Ginzburg-Landau-Wilson theory for the classical nematic phase transition in liquid crystals, which exhibits a fixed point if and only if the dimension p of the tensor order parameter is $p < p_c$ with $p_c = 4$ to leading order in the related $\epsilon = 6 - d$ expansion [39]. However, the existence of the fermionic fixed point (F in Fig. 2) remains unaffected by this, and we find the nontrivial solution for $c = \mathcal{O}(\epsilon^{6/5})$:

$$\frac{\lambda_\pm^*}{c^{*1/4}} = \pm \frac{1}{3}\sqrt{\epsilon}, \quad \frac{g_\pm^*}{c^{*1/12}} = \pm \sqrt{\frac{3}{2}}\sqrt{\epsilon}, \quad (\text{E9})$$

where albeit λ_\pm^* and g_\pm^* now have the same sign. Examination of the stability matrix shows that the fermionic fixed point now exhibits a second relevant direction in direction of λ . This again reflects the fact that for the four-dimensional tensor order parameter there is no purely bosonic fixed point at $g = 0$ and $\lambda \neq 0$ and the flow in the direction of λ is unbounded. In agreement with the discussion of the classical nematic phase transition [39] we thus believe that the physical situation in $d = 3$ is more accurately described by the calculation directly in $d = 3$ as presented in the main text, which gives the stable fermionic fixed point with g^* and λ^* being of opposite sign.

In any case, to the leading order we find for the $d = 4$ calculation precisely the same values for the critical exponents at the fermionic fixed point as in the main text [cf. Eqs. (52) and (55)],

$$\eta_\psi = \mathcal{O}(\epsilon^{6/5}), \quad \eta_\phi = \epsilon + \mathcal{O}(\epsilon^{6/5}), \quad z = 2 + \mathcal{O}(\epsilon^{6/5}), \quad (\text{E10})$$

and

$$1/\nu = 2 + 5\epsilon + \mathcal{O}(\epsilon^{6/5}). \quad (\text{E11})$$

-
- [1] See, F. Parisen Toldin, M. Hohenadler, F. F. Assaad, and I. F. Herbut, Fermionic quantum criticality in honeycomb and π -flux hubbard models, *Phys. Rev. B* **91**, 165108 (2015), and references therein.
- [2] See, for example, V. Cvetković, R. E. Throckmorton, and O. Vafek, Electronic multicriticality in bilayer graphene, *Phys. Rev. B* **86**, 075467 (2012), and references therein.
- [3] K. Sun, H. Yao, E. Fradkin, and S. A. Kivelson, Topological insulators and nematic phases from spontaneous symmetry breaking in 2D: Fermi systems with a quadratic band crossing, *Phys. Rev. Lett.* **103**, 046811 (2009).
- [4] B. Dóra, I. F. Herbut, and R. Moessner, Occurrence of nematic, topological, and Berry phases when a flat and a parabolic band touch, *Phys. Rev. B* **90**, 045310 (2014).
- [5] W. Witczak-Krempa, G. Chen, Y. B. Kim, and L. Balents, Correlated quantum phenomena in the strong spin-orbit regime, *Ann. Rev. Cond. Matt. Phys.* **5**, 57 (2014).
- [6] A. A. Abrikosov, Calculation of critical indices for zero-gap semiconductors, *Sov. Phys. JETP* **39**, 709 (1974).
- [7] E.-G. Moon, C. Xu, Y. B. Kim, and L. Balents, Non-Fermi-liquid and topological states with strong spin-orbit coupling, *Phys. Rev. Lett.* **111**, 206401 (2013).
- [8] I. F. Herbut and L. Janssen, Topological Mott insulator in three-dimensional systems with quadratic band touching, *Phys. Rev. Lett.* **113**, 106401 (2014).
- [9] I. F. Herbut and Z. Tešanović, Critical fluctuations in superconductors and the magnetic field penetration depth, *Phys. Rev. Lett.* **76**, 4588 (1996).
- [10] I. F. Herbut and Z. Tešanović, Herbut and Tešanović reply, *Phys. Rev. Lett.* **78**, 980 (1997).
- [11] K. Kaveh and I. F. Herbut, Chiral symmetry breaking in three-dimensional quantum electrodynamics in the presence of irrelevant interactions: A renormalization group study, *Phys. Rev. B* **71**, 184519 (2005).
- [12] H. Gies, and J. Jaeckel, Chiral phase structure of QCD with many flavors, *Eur. Phys. J. C* **46**, 433 (2006).
- [13] D. B. Kaplan, J.-W. Lee, D. T. Son, and M. A. Stephanov, Conformality lost, *Phys. Rev. D* **80**, 125005 (2009).
- [14] L. Fu and C. L. Kane, Topological insulators with inversion symmetry, *Phys. Rev. B* **76**, 045302 (2007).
- [15] S. Raghu, X.-L. Qi, C. Honerkamp, and S.-C. Zhang, Topological Mott insulators, *Phys. Rev. Lett.* **100**, 156401 (2008).
- [16] M. Daghofer and M. Hohenadler, Phases of correlated spinless fermions on the honeycomb lattice, *Phys. Rev. B* **89**, 035103 (2014).
- [17] A. G. Grushin, E. V. Castro, A. Cortijo, F. de Juan, M. A. H. Vozmediano, and B. Valenzuela, Charge instabilities and topological phases in the extended hubbard model on the honeycomb lattice with enlarged unit cell, *Phys. Rev. B* **87**, 085136 (2013).
- [18] T. Duric, N. Chancellor, and I. F. Herbut, Interaction-induced anomalous quantum hall state on the honeycomb lattice, *Phys. Rev. B* **89**, 165123 (2014).
- [19] I. F. Herbut, Interactions and phase transitions on graphene's honeycomb lattice, *Phys. Rev. Lett.* **97**, 146401 (2006).
- [20] I. F. Herbut, V. Juričić, and B. Roy, Theory of interacting electrons on the honeycomb lattice, *Phys. Rev. B* **79**, 085116 (2009).
- [21] I. F. Herbut, V. Juričić, and O. Vafek, Relativistic Mott criticality in graphene, *Phys. Rev. B* **80**, 075432 (2009).
- [22] S. Ryu, C. Mudry, C.-Y. Hou, and C. Chamon, Masses in graphenelike two-dimensional electronic systems: Topological defects in order parameters and their fractional exchange statistics, *Phys. Rev. B* **80**, 205319 (2009).
- [23] I. F. Herbut, Isospin of topological defects in Dirac systems, *Phys. Rev. B* **85**, 085304 (2012).
- [24] P. M. Chaikin and T. C. Lubensky, *Principles of Condensed Matter Physics* (Cambridge University Press, Cambridge, 1995).
- [25] I. F. Herbut, Time reversal, fermion doubling, and the masses of lattice Dirac fermions in three dimensions, *Phys. Rev. B* **83**, 245445 (2011).
- [26] J. M. Luttinger, Quantum theory of cyclotron resonance in semiconductors: General theory, *Phys. Rev.* **102**, 1030 (1956).
- [27] S. Murakami, N. Nagaosa, S.-C. Zhang, SU(2) non-Abelian holonomy and dissipationless spin current in semiconductors, *Phys. Rev. B* **69**, 235206 (2004).
- [28] This follows from the table of Clifford algebra representations presented in Ref. [23].
- [29] V. Oganesyan, S. A. Kivelson, and E. Fradkin, Quantum theory of a nematic Fermi fluid, *Phys. Rev. B* **64**, 195109 (2001).
- [30] M. A. Metlitski and S. Sachdev, Quantum phase transitions of metals in two spatial dimensions. I. Ising-nematic order, *Phys. Rev. B* **82**, 075127 (2010).
- [31] T. Holder and W. Metzner, Anomalous dynamical scaling from nematic and U(1)-gauge field fluctuations in two dimensional metals, [arXiv:1503.05089](https://arxiv.org/abs/1503.05089) [cond-mat.str-el] (2015).
- [32] E. Fradkin, S. A. Kivelson, M. J. Lawler, J. P. Eisenstein, and A. P. MacKenzie, Nematic Fermi fluids in condensed matter physics, *Ann. Rev. Cond. Matt. Phys.* **1**, 153 (2010).
- [33] T. Meng, A. Rosch, and M. Garst, Quantum criticality with multiple dynamics, *Phys. Rev. B* **86**, 125107 (2012).
- [34] L. Savary, E.-G. Moon, and L. Balents, New type of quantum criticality in the pyrochlore iridates, *Phys. Rev. X* **4**, 041027 (2014).
- [35] B. J. Roman and A. W. Ewald, Stress-induced band gap and related phenomena in gray tin, *Phys. Rev. B* **5**, 3914 (1972).
- [36] For the uniaxial states we can in fact evaluate the integral in E_{MF} [Eq. (30)] analytically for any ϕ : For $\xi = 0$, for instance, we find $E_{\text{MF}}(\Lambda^2\phi/g, 0)/\Lambda^5 = \frac{r}{2\Lambda g^2}\phi^2 - \frac{4\pi}{(2\pi)^3}[-\frac{1}{6} + \frac{1}{4}\phi +$

$\frac{1}{3}\phi^2 - \frac{\pi}{8}\phi^{5/2} + \frac{2-3\phi+6\phi^2}{12\sqrt{3}\phi} \operatorname{artanh} \frac{\sqrt{3}\phi}{1+\phi} + \frac{1}{8}\phi^{5/2} \arctan \sqrt{\frac{\phi}{(1-\phi)^2}} + \frac{5}{48\sqrt{3}}\phi^{5/2} \ln \frac{(1-\sqrt{3}\phi+\phi^2)^2}{1-\phi+\phi^2}$], showing that $E_{\text{MF}}(\phi)$ at larger ϕ does not exhibit a second minimum and that the mean-field transition is indeed continuous, as stated in the text.

[37] I. Herbut, *A Modern Approach to Critical Phenomena* (Cambridge University Press, Cambridge, 2007).
 [38] L. Janssen and I. F. Herbut, Antiferromagnetic critical point on graphene's honeycomb lattice: A functional renormalization

group approach, *Phys. Rev. B* **89**, 205403 (2014), and references therein.

[39] R. G. Priest and T. C. Lubensky, Critical properties of two tensor models with application to the percolation problem, *Phys. Rev. B* **13**, 4159 (1976).
 [40] L. Janssen and I. F. Herbut (unpublished).
 [41] F. T. Hioe and J. H. Eberly, N -Level coherence vector and higher conservation laws in quantum optics and quantum mechanics, *Phys. Rev. Lett.* **47**, 838 (1981).